ELSEVIER

PII: S0308-0161(96)00034-8

Int. J. Pres. Ves. & Piping **70** (1997) 223–236

0308-0161/97/$17.00

Probabilistic fracture analysis of cracked pipes with circumferential flaws

S. Rahman

Department of Mechanical Engineering, The University of Iowa, Iowa City, Iowa 52242, USA

(Received 14 December 1995; revised 17 July 1996; accepted 29 July 1996)

This paper describes the development of a probabilistic fracture-mechanics model for analyzing circumferential through-walled-cracked pipes subject to bending loads. It involves elastic–plastic finite element analysis for estimating energy release rates, J-tearing theory for characterizing ductile fracture, and standard structural reliability methods for conducting probabilistic analysis. The evaluation of the J-integral is based on the deformation theory of plasticity and power-law idealizations of stress–strain and fracture toughness curves. This allows J to be expressed in terms of non-dimensional influence functions (F- and h_1-functions) that depend on crack size, pipe geometry, and material hardening constant. New equations were developed to represent these functions. Both analytical and simulation methods were formulated to determine the probabilistic characteristics of J. The same methods were used later to predict the failure probability of pipes as a function of applied load. Numerical examples are provided to illustrate the proposed methodology. The validity of the J-integral based on the proposed equations for predicting the crack driving force in a through-wall-cracked pipe was evaluated by comparison with available results in the current literature. Probability densities of the J-integral were predicted as a function of applied loads. Failure probabilities corresponding to three different performance criteria were evaluated for stainless steel nuclear piping from a boiling water reactor plant. The results suggest that large differences may exist in the failure probability estimates produced by these performance criteria. © 1997 Elsevier Science Ltd. All rights reserved.

1 INTRODUCTION

Many structural systems are comprised of piping systems which can be found in nuclear power plants, off-shore drilling platforms, gas transmission lines, fossil power generation plants and others. The unavoidable existence of cracks in some components may lead to increased safety concerns about the loss of structural strength and possibly failure of structural systems. The traditional approach to safety assessment and design lies in a deterministic model which invariably involves a large safety factor usually assigned from heuristic and somewhat arbitrary decisions. This approach has almost certainly been reinforced by the very large extent to which conventional engineering design is codified and the lack of feedback about the actual performance of the structure. Use of large safety factors can lead to the view that 'absolute' safety can be achieved. Absolute safety is of course undesirable if not unobtainable, since it could only be approached by deploying infinite resources.

A realistic evaluation of structural performance can be conducted only if the uncertainty in structural loads, flaw sizes, and material properties, and hence responses are taken into consideration. Typical response parameters of piping systems that undergo plastic deformation due to applied loads are the J-integral, crack tip opening displacement, and others. While the load and the resistance are not deterministic, they nevertheless show statistical regularity and the statistical information, which are necessary to describe their probability laws, and are available from the existing literature. For example, the material properties of base and weld metals typically used in nuclear piping can be obtained from the PIFRAC database,[1] the Degraded Piping Program[2] and the International Piping Integrity Research Group (IPIRG) Programs,[3] and others.[4–6] A systematic search of the above database from these research programs can provide a wealth of data for statistical characterization of the strength (stress–strain curve) and the toughness (J-resistance) properties of typical pipe materials. These suggest that the probability

theory and structural reliability methods can be applied to assess performance of piping and piping welds subjected to in-service (normal operational loads) and extreme (seismic loads) loading environments.

This paper presents a stochastic fracture-mechanics model to evaluate the structural performance of circumferential through-walled-cracked (TWC) pipes subject to bending loads. The model involves; (1) elastic–plastic finite-element analysis for estimating the energy release rate; (2) J-tearing theory for characterizing ductile fracture; and (3) standard methods of structural reliability theory for conducting probabilistic analysis. The evaluation of the J-integral is based on the deformation theory of plasticity and constitutive law characterized by power-law equation for stress–strain curve. This permits the J-integral to be expressed in terms of non-dimensional influence functions that depend on crack geometry, pipe geometry, and material hardening constant. Closed-form equations were developed for these functions (and hence, J) based on recent results of elastic–plastic finite element analysis. This makes the subsequent stochastic analysis computationally feasible to evaluate probabilistic characteristics of the J-integral and the failure loads. Both analytical and computational methods e.g. first- and second-order reliability methods and simulation methods, e.g. Monte Carlo simulation, and importance sampling were formulated to determine the relevant probability measures for pipe fracture evaluations. Numerical examples from nuclear plant piping are presented to illustrate the proposed methodology.

2 ELASTIC–PLASTIC FRACTURE ANALYSIS

It is now well established that elastic–plastic fracture mechanics (EPFM) provides more realistic measures of fracture behavior of cracked piping systems when compared with the elastic methods. The use of EPFM becomes almost necessary for piping materials with high toughness and low strength which generally undergo extensive plastic deformation around a crack tip. Recent analytical, experimental and computational studies on this subject indicate that the energy release rate (also known as the J-integral) and crack tip opening displacement (CTOD) are the most viable fracture parameters for characterizing crack initiation, stable crack growth, and subsequent instability in ductile materials.[7,8] This clearly suggests that the global parameters like J and/or CTOD can be conveniently used to assess structural integrity for both leak-before-break and in-service flaw acceptance criteria in degraded piping systems. It is, however, noted that the parameter J still possesses some theoretical limitations. For example, the Hutchinson–Rice–Rosengren (HRR) singular field,[9,10] may not be valid in the case of certain amounts of crack extension where J ceases to act as amplifier for this singular field. Nevertheless, possible error is considered tolerable if the relative amount of crack extension stays within a certain limit and if elastic unloading and non-proportional plastic loading zones around a crack tip are surrounded by a much larger zone of nearly proportional loading controlled by the HRR field. Under this condition of J-dominance, both the onset and limited amount of crack growth can be correlated to the critical values of J and the J–resistance curve, respectively.[11]

Consider a pipe, shown in Fig. 1, which has mean radius R, wall thickness t, and a circumferential through-wall crack of total angle 2θ and mean length $2a = 2R\theta$. It is assumed that the constitutive law characterizing the material's stress–strain response can be represented by the well-known Ramberg–Osgood model

$$\frac{\varepsilon}{\varepsilon_0} = \frac{\sigma}{\sigma_0} = \alpha\left(\frac{\sigma}{\sigma_0}\right)^n \tag{1}$$

in which σ_0 is a reference stress, which can be arbitrary, but is usually assumed to be the yield stress, E is the modulus of elasticity, $\varepsilon_0 = \sigma_0/E$ is the associated reference strain, and α and n are model parameters usually chosen from best fit of actual laboratory data. Also, the J-resistance curve from the compact tension specimen is deemed to be adequately characterized by a power-law equation

$$J_R(\Delta a) = J_{Ic} + C\left(\frac{\Delta a}{k}\right)^m \tag{2}$$

in which $\Delta a = R\Delta\theta$ is the crack length extension during crack growth, J_{Ic} is the fracture toughness at crack initiation, and C and m are model parameters also obtained from best fit of experimental data. In eqn (2), k is a dummy parameter with a value of 1 introduced here only to dimensionalize C (e.g. when Δa is expressed in mm, if $k = 1$ mm, C has the same dimensions as J). Note that 'Δa' here is the physical

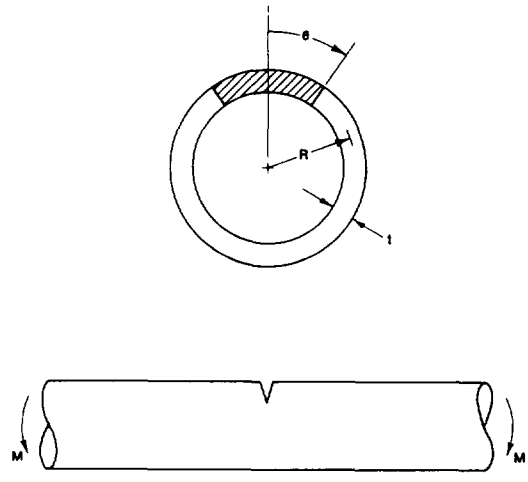

Fig. 1. A pipe with a circumferential through-wall crack subject to pure bending.

crack extension, i.e. without blunting. This is because blunting is automatically accounted for in the pipe estimation schemes as well as finite element analysis.

2.1 The *J*-integral

The *J*-integral defines the amplitude of the HRR singularity field, just as the stress intensity factor characterizes the amplitude of the stress field in linear-elastic fracture mechanics (LEFM). Thus *J* completely describes the conditions within the plastic zone. A cracked structure in small-scale yielding has two singularity-dominated zones: one in the elastic region, where stress varies as $r^{-1/2}$ and one in the plastic zone, where stress varies as $r^{-(1/n+1)}$ (r is a polar co-ordinate with crack tip as the origin). In EPFM, the latter often persists long after the linear elastic singularity zone has been destroyed by crack tip plasticity.

Under elastic–plastic conditions and deformation theory of plasticity when the stress–strain curve is modeled by eqn (1), the total crack driving force J can be obtained by adding the elastic component J_e and the plastic component J_p, i.e.

$$J = J_e + J_p. \tag{3}$$

For a TWC pipe under pure bending, closed-form expressions can be developed for both J_e and J_p. They are described below.

2.1.1 Elastic solution

The elastic component J_e is given by Refs 12–14

$$J_e = \frac{K_i^2}{E} \tag{4}$$

where K_i is the mode-i stress intensity factor in which the plane stress condition is assumed for a TWC pipe. From LEFM theory, K_i can be obtained as

$$K_i = \frac{M}{\pi R^2 t} F\left(\frac{\theta}{\pi}, \frac{R}{t}\right)\sqrt{\pi R\theta} \tag{5}$$

where $F(\theta/\pi, R/t)$ is a dimensionless function that depends on pipe and crack geometry. Hence, the elastic J is

$$J_e = \frac{\theta}{\pi} F\left(\frac{\theta}{\pi}, \frac{R}{t}\right)^2 \frac{M^2}{ER^3t^2} \tag{6}$$

2.1.2 Plastic solution

For the J controlled condition, the loading must be proportional, i.e. the local stresses must increase in proportion to the remote applied load, M. Therefore, for the pipe crack problem, the plastic J can be expressed as[12–14]

$$J_p = \frac{\alpha\sigma_0^2}{E} R\theta\left(1 - \frac{\theta}{\pi}\right) h_1\left(\frac{\theta}{\pi}, n, \frac{R}{t}\right)\left[\frac{M}{M_0}\right]^{n+1} \tag{7}$$

in which $h_1(\theta/\pi, n, R/t)$ is another dimensionless function that depends on pipe geometry, crack geometry, and material constant, and

$$M_0 = 4\sigma_0 R^2 t\left[\cos\frac{\theta}{2} - \frac{1}{2}\sin\theta\right] \tag{8}$$

is a conveniently defined reference load that represents the limit-load for a TWC pipe under pure bending if σ_0 is the collapse stress. Thus, for a given TWC pipe if F and h_1 are known, the crack driving force J can be predicted readily.

2.2 Evaluation of *F*- and h_1-functions

2.2.1 Finite element analysis

The influence functions, $F(\theta/\pi, R/t)$ and $h_1(\theta/\pi, n, R/t)$, can be computed by using the finite element method (FEM). Computations of this kind for through-wall-cracked pipes were first reported by Kumar *et al.*[13,14] The finite element analyses by Kumar *et al.*[13,14] involved 9-noded shell elements with three displacement and two rotational degrees of freedom at each node. The elements had only one node in the thickness direction. No special elements were needed to account for plastic incompressibility since the TWC pipe under tension or bending is essentially a plane stress problem.[13,14] J was calculated by the virtual crack extension technique.[13,14] In Kumar *et al.*[13,14] these influence functions are cataloged at several discrete values of parameters θ/π, n and R/t. For a given pipe with arbitrary values of these parameters, the corresponding F- and h_1-functions can be determined via interpolation or extrapolation of these tabulated values.

In a recent study at Battelle, these influence functions were examined to determine their adequacy for flaw evaluation of pipes with circumferential through-wall cracks. From preliminary evaluation, it was found that: (1) the compiled values of h_1, and hence J_p, were too large especially when the material hardening exponent n is large and/or the crack size θ/π is small; (2) for small crack sizes, the pipe rotations due to cracking were negative for both elastic and plastic solutions; and (3) no solutions were made available for $n = 10$ and some of the $n = 7$ cases due to reported numerical difficulties. Some of these difficulties may be due to the use of simple 9-noded shell elements that could have produced overly stiff results.[15,16] In consequence, the above influence functions were recomputed with particular attention to pipes with short through-wall cracks (e.g. when $\theta/\pi \leq 1/8$).[16] In these new calculations several load

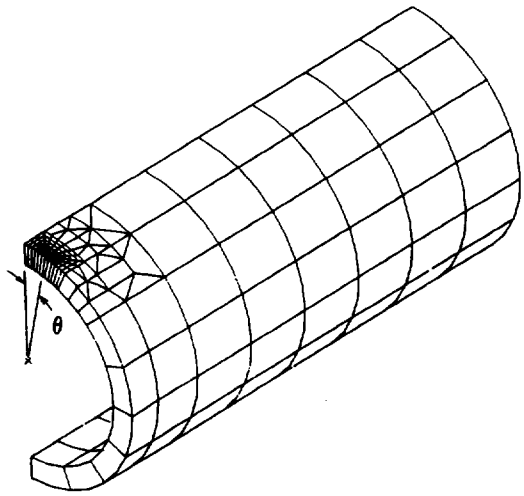

Fig. 2. Finite element idealization for a quarter pipe with a through-wall crack.

cases, such as tension, bending, and combined bending and tension, were considered. Figure 2 shows a typical finite element mesh for a TWC pipe. Due to symmetry, only a quarter of the pipe needed to be modeled. In all cases, 20-noded isoparametric brick elements were used with adequate refinement at the crack tip. Only one element through the pipe wall thickness was used and as such, the results should be viewed as average values through the pipe wall. The elastic solutions were developed using the elastic properties of the pipe. A deformation theory of plasticity algorithm in the ABAQUS finite element code[17] was used to generate the plastic solution. A reduced 2×2 Gauss quadrature integration rule was utilized. J was calculated by the contour integral definition.[15–18] The calculations were carried out for $\theta/\pi = 1/16$, $1/8$, $1/4$ and $1/2$, $n = 1$, 2, 3, 5, 7 and 10, and $R/t = 5$, 10 and 20. No numerical difficulties were encountered. Further details are available in the papers by Brust *et al.*[8,16]

2.2.2 Analytic approximations

Following explicit finite element (ABAQUS) calculations of F- and h_1-functions at the pre-determined values of θ/π, n and R/t, multi-variate response surface approximations were recently developed by the author.[19] The proposed equations for $F(\theta/\pi, R/t)$ and $h_1(\theta/\pi, n, R/t)$ are

$$F\left(\frac{\theta}{\pi}, \frac{R}{t}\right) = 1 + \{A_1 \quad A_2 \quad A_3\} \times \begin{Bmatrix} \left(\frac{\theta}{\pi}\right)^{1.5} \\ \left(\frac{\theta}{\pi}\right)^{2.5} \\ \left(\frac{\theta}{\pi}\right)^{3.5} \end{Bmatrix} \{B_1 \quad B_2 \quad B_3 \quad B_4\} \begin{Bmatrix} 1 \\ \left(\frac{R}{t}\right) \\ \left(\frac{R}{t}\right)^2 \\ \left(\frac{R}{t}\right)^3 \end{Bmatrix} \quad (9)$$

$$h_1\left(\frac{\theta}{\pi}, n, \frac{R}{t}\right) = \left\{1 \left(\frac{\theta}{\pi}\right) \left(\frac{\theta}{\pi}\right)^2 \left(\frac{\theta}{\pi}\right)^3\right\} \times \begin{bmatrix} C_{00} & C_{10} & C_{20} & C_{30} \\ C_{01} & C_{11} & C_{21} & C_{31} \\ C_{02} & C_{12} & C_{22} & C_{32} \\ C_{03} & C_{13} & C_{23} & C_{33} \end{bmatrix} \begin{Bmatrix} 1 \\ n \\ n^2 \\ n^3 \end{Bmatrix} \quad (10)$$

where the coefficients A_i $(i = 1, 2, 3)$, B_i $(i = 1, 2, 3, 4)$, and C_{ij} $(i, j = 0, 1, 2, 3)$ were calculated from the best-fit of FEM results. Note that the coefficients A_i and B_i are both constant while the coefficient C_{ij} depends on the R/t ratio. The values of these coefficients are provided in Appendix A. Using these values, Figs 3 and 4 show the surface plots of F- and h_1-functions (for $R/t = 10$) defined by eqns (9) and (10), respectively. The points with the droplines in these figures represent the numerical values from the ABAQUS finite element calculations.[16–18] Further details and similar plots of h_1-functions for other values of R/t are available in Rahman.[19]

2.2.3 Comparisons with other solutions

Other solutions of F- and h_1-functions available in the literature were compared with eqns (9) and (10) to evaluate their adequacy. They involved analytical solutions by Sanders' energy release rate (elastic) formula,[20,21] analytical solutions by Klecker *et al.*[22] and Zahoor,[23] and extensive finite-element calculations by Kumar *et al.*,[13,14] and Brust *et al.*[16,18] Figure 5 shows the comparisons of proposed F with these solutions as a function of crack size θ/π for $R/t = 5$, 10 and 20. As expected, eqn (9) agrees very well with all FEM calculations by Brust *et al.* There is little difference between the FEM results by Brust *et al.* and Kumar *et al.* when the crack size is smaller (e.g. $\theta/\pi \leq 1/8$). However, for large crack size and large $R/t = 20$, the FEM values of F produced by Brust *et al.* are slightly greater than those generated by Kumar *et al.* The Sanders' solutions provide accurate results for large

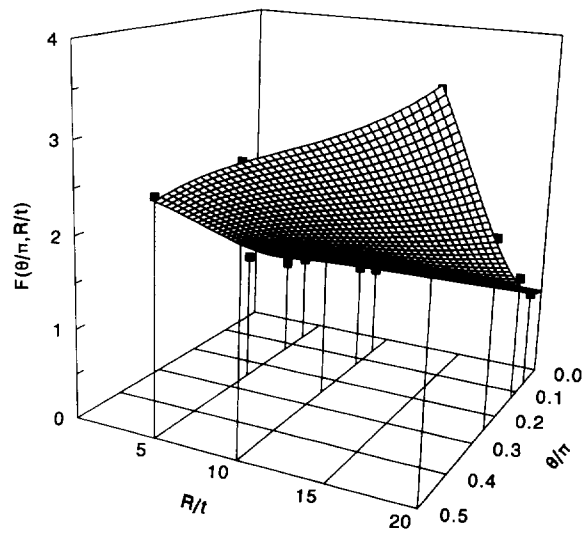

Fig. 3. Surface plot of proposed F-function.

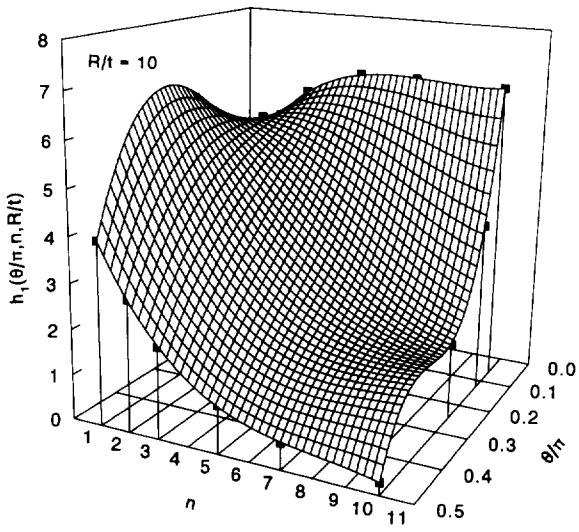

Fig. 4. Surface plot of proposed h_1-function for $R/t = 10$.

cracks, but can be overly unconservative for small cracks. In the limit when θ/π approaches zero, the Sanders' solutions do not converge to unity. The solutions by Klecker *et al.*, which were developed based on Sanders' solutions with corrections for small cracks, are closer to the Kumar *et al.* solutions. The

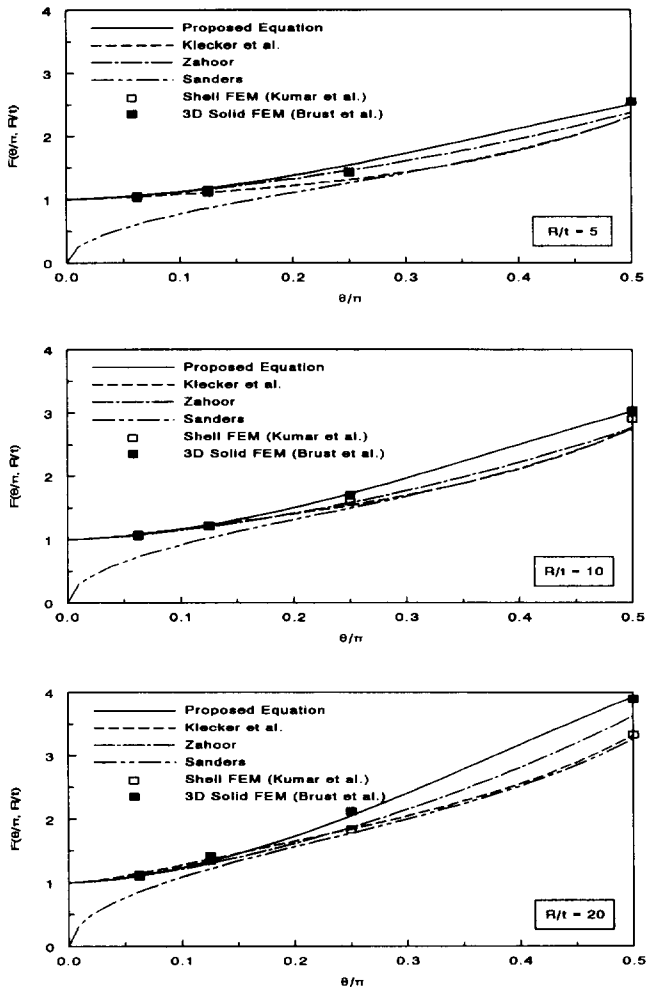

Fig. 5. Comparisons of f-functions by various methods.

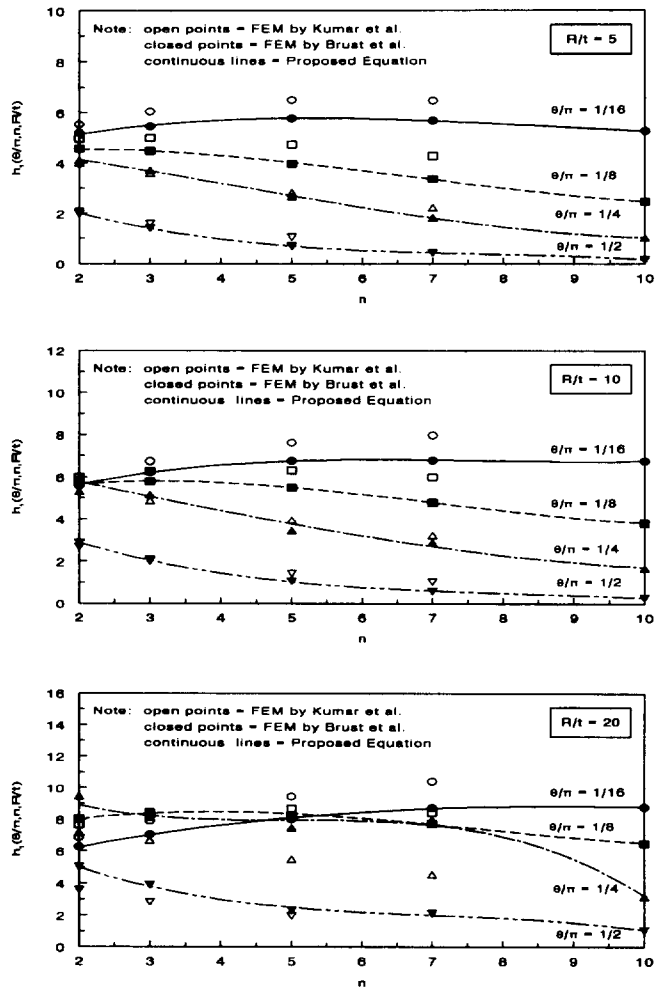

Fig. 6. Comparisons of h_1-functions by various methods.

solutions by Zahoor appear to fall in between the FEM results of Brust *et al.* and Kumar *et al.*

Figure 6 shows similar plots of h_1 as a function of material constant n for several cases of crack size $\theta/\pi = 1/16$, 1/8, 1/4 and 1/2, and $R/t = 5$, 10 and 20 by various methods. As before, the solutions include finite element calculations by Brust *et al.*[16,18] and Kumar *et al.*[13,14] However, no analytical solutions were available for calculating h_1 due to the complexity of the problem. From Fig. 6, there are some differences between the FEM results of Brust *et al.* and Kumar *et al.* when the crack size is small (e.g. $\theta/\pi \leq 1/8$) and/or material hardening exponent n is large (e.g. $n \geq 5$). In those cases, the values of h_1 produced by Kumar *et al.* are always greater than those generated by Brust *et al.* Hence, for short TWC cracked pipes with ferritic steel or ferritic/austenitic welds (which are usually associated with large n), the prediction of load-carrying capacity based on Kumar *et al.* influence functions can be somewhat conservative. This is consistent with the author's past experience during analyses of full-scale pipe fracture experiments.[18,24–26] Also, for large R/t (e.g. $R/t = 20$), some differences may also exist between these FEM

solutions. Further details on the comparisons of results for other influence functions for crack-opening displacement, pipe displacement and pipe rotation are discussed in Brust *et al.*[16,18]

The F- and h_1-functions developed by the author (eqns (9) and (10)) should be applicable for $1/16 \leq \theta/\pi \leq 1/2$, $1 \leq n \leq 10$, and $5 \leq R/t \leq 20$. For the parameter values outside these ranges, they were not verified in this study since no corresponding FEM results were available. Also, the adequacy of these functions should be further evaluated by comparing with more elastic–plastic FEM results when available.

3 FAILURE LOAD

In order to evaluate structural integrity, it is required to know the load-carrying capacity of a piping system. These are several means by which it can be estimated. They are based on various definitions of failure criteria such as, initiation of crack growth and unstable crack growth in elastic–plastic fracture mechanics, and the net-section collapse in limit-load analysis. They are briefly described below.

3.1 Initiation load

The initiation load M_i can be defined as the bending moment which corresponds to initiation of crack growth in a pipe. If J is a relevant crack driving force, it can be estimated by solving the following nonlinear equation

$$f(M_i) = J(M_i, a) - J_{Ic} = 0 \tag{11}$$

in which $J(M_i, a)$ is the energy release rate (i.e. J-integral) for load M_i and crack size $a = R\theta$, which can be obtained from eqns (3), (6) and (7), and J_{Ic} is the plane strain mode-I fracture toughness at crack initiation. J_{Ic} can be determined from standard compact tension test at the laboratory.[1–6,24] Standard numerical methods, such as the bisection method, Newton–Raphson method, and others, can be applied to solve eqn (11).[27]

3.2 Maximum load

In applications of nonlinear fracture mechanics, particularly for nuclear power plants, the J-tearing theory is a very prominent concept for calculating the maximum load-carrying capacity of a pipe. It is based on the fact that fracture instability can occur after some amount of stable crack growth in tough and ductile materials with an attendant higher applied load level at fracture. Let J and J_R denote the crack driving force and toughness of a ductile piping material as a function of load and crack size. The limit state characterizing fracture instability based on J-tearing theory is given by

$$f_1(M_{max}, a^*) = J(M_{max}, a^*) - J_R(a^* - a) = 0 \tag{12}$$

and

$$f_2(M_{max}, a^*) = \frac{\partial J}{\partial a}(M_{max}, a^*) - \frac{dJ_R}{da}(a^* - a) = 0 \tag{13}$$

where M_{max} and a^* represent load and half the crack length when crack growth becomes unstable. Equations (12) and (13) are two nonlinear simultaneous equations with the independent variables M_{max} and a^*. Once again, they can be solved by standard methods, such as the Newton–Raphson method.[27]

3.3 Net-section collapse load

The net-section collapse analysis is a simple, straightforward failure prediction method for TWC pipes in pure bending. In this analysis, it is assumed that: (1) the failure load occurs when the pipe section containing the crack becomes fully plastic; (2) there is insignificant crack growth from crack initiation to failure; and (3) the toughness of the material is sufficiently high so that failure is governed by the strength of materials (i.e. the flow stress or collapse stress). The collapse stress is a value between the yield and ultimate strengths of a material and represents an average critical net-section stress throughout the remaining ligament of the structure. Based on these assumptions, the net-section collapse load M_{nsc} is given by[28]

$$M_{nsc} = 4\sigma_f R^2 t\left(\cos\frac{\theta}{2} - \frac{1}{2}\sin\theta\right) \tag{14}$$

where σ_f is the flow stress or the collapse stress. In this paper, σ_f is assumed to be the average of yield and ultimate strengths of the pipe material.

4 RANDOM PARAMETERS AND SYSTEM RESPONSE

Consider a cracked pipe with uncertain mechanical and geometric characteristics that is subject to random loads. Denote by $\mathbf{X}$ an N-dimensional random vector with components $X_1, X_2, \ldots, X_N$ characterizing uncertainty in the system and load parameters. For example, when a TWC pipe is considered, the possible random components are: crack size θ/π, pipe radius-to-thickness (R/t) ratio, elastic modulus E, basic strength parameters σ_y and σ_u, Ramberg–Osgood constitutive parameters α and n, fracture toughness parameters J_{Ic}, C and m, and applied

bending moment M. All or some of these variables can be modeled as random variables. Hence, any relevant response, such as the J-integral, should be evaluated by the probability

$$F_J(j_0) \stackrel{\text{def}}{=} Pr[J(\mathbf{X}) < j_0] \stackrel{\text{def}}{=} \int_{J(\mathbf{x})<j_0} f_{\mathbf{X}}(\mathbf{x})\,\mathrm{d}\mathbf{x} \qquad (15)$$

or the probability density $f_J(j_0) = \mathrm{d}F_J(j_0)/\mathrm{d}j_0$ where $F_J(j_0)$ is the cumulative probability distribution function of J and $f_{\mathbf{X}}(\mathbf{x})$ is the known joint probability density function of random vector $\mathbf{X}$.

The above fracture parameter J can also be applied to determine the load-carrying capacity of TWC pipes. Several fracture criteria based on this J-integral parameter and net-section collapse are discussed in Section 3. In a generic sense, let $M_f(\mathbf{X})$ denote the failure moment for a given TWC pipe under pure bending. Note that $M_f(\mathbf{X})$ is always random because it depends on input vector $\mathbf{X}$ which is random. It can be evaluated when a relevant crack driving force from deterministic fracture (e.g. J-integral from finite element analysis or eqns (9) and (10)) and an appropriate fracture criteria (e.g. eqn (11) or eqns (12) and (13)) are known. Suppose that the design requires $M_f(\mathbf{X})$ to be always greater than the applied load M (M can be random as well). This requirement cannot be satisfied with certainty because both the system and the load parameters are uncertain. Hence, the performance of the pipe should be evaluated by the reliability P_S or its complement, the probability of failure, P_F ($P_S = 1 - P_F$) defined as

$$P_F \stackrel{\text{def}}{=} Pr[g(\mathbf{X}) < 0] \stackrel{\text{def}}{=} \int_{g(\mathbf{x})<0} f_{\mathbf{X}}(\mathbf{x})\,\mathrm{d}\mathbf{x} \qquad (16)$$

where the $g(\mathbf{X})$ is the performance function given by

$$g(\mathbf{X}) = \mathbf{M}_f - M$$
$$= S(\sigma_y, \sigma_u, \alpha, n, J_{Ic}, C, m, \theta/\pi, R/t, E) - M \qquad (17)$$

in which S is a function (implicit) of random parameters characterizing the pipe's structural resistance (only the random arguments are shown in eqn (17)). A wide variety of failure probability, defined by eqn (16), can be evaluated if the appropriate fracture criterion is known. For example, when $M_f(\mathbf{X})$ is equal to the initiation load $M_i(\mathbf{X})$, P_F in eqn (16) corresponds to the probability of initiation of crack growth which provides a conservative estimate of the pipe's structural performance. A more realistic evaluation of a pipe's reliability can be evaluated if $M_f(\mathbf{X})$ is equal to the maximum load $M_{max}(\mathbf{X})$ (which allows the crack to grow until it becomes unstable) in which case P_F represents failure probability due to the exceedance of the pipe's maximum load-carrying capacity. When EPFM-based failure criteria are not necessary, a simple performance function based on limit-load analysis [i.e. $M_f(\mathbf{X}) = M_{nsc}(\mathbf{X})$] can also be used to determine failure probability of pipes.

Numerical efforts are often required to compute $M_f(\mathbf{X})$ particularly when $M_f(\mathbf{X}) = M_i(\mathbf{X})$ or $M_{max}(\mathbf{X})$. This is true in spite of analytical representations of F- and h_1-functions to compute J_e and J_p, respectively. In this paper, the Newton–Raphson method is used to solve for $M_i(\mathbf{X})$ and $M_{max}(\mathbf{X})$.

5 STRUCTURAL RELIABILITY ANALYSIS

The generic expression for both probabilities in eqns (15) and (16) involves multi-dimensional probability integration for their evaluation. In this regard, standard reliability methods, such as first- and second-order reliability methods (FORM/SORM)[19,29–34] and simulation methods, such as importance sampling (IS),[19,35–40] Monte Carlo Simulation (MCS),[19,41] and others, can be applied to compute these probabilities. Some of these methods have been successfully applied to various probabilistic fracture-mechanics evaluations.[42–44] In this paper, FORM/SORM, importance sampling and MCS methods are used for structural reliability analysis. They are briefly described here to compute the probability of failure P_F in eqn (16) assuming a generic N-dimensional random vector $\mathbf{X}$ and the performance function $g(\mathbf{x})$ defined by eqn (17). The same methods can be applied to determine the probability $F_J(j_0)$ defined by eqn (15).

5.1 First- and second-order reliability methods (FORM/SORM)

First- and second-order reliability methods are based on linear (first-order) and quadratic (second-order) approximations of the limit state surface $g(\mathbf{x}) = 0$ tangential to the closest point of the surface to the origin of the space. The determination of this point involves nonlinear constrained optimization and is performed in the standard Gaussian image of the original space. The FORM/SORM algorithms involve several steps. First, the space of uncertain parameters $\mathbf{x}$ is transformed into a new N-dimensional space $\mathbf{u}$ consisting of independent standard Gaussian variables. The original limit state $g(\mathbf{x}) = 0$ then becomes mapped into the new limit stage $g_U(\mathbf{u}) = 0$ in the $\mathbf{u}$ space. Second, the point on the limit stage $g_U(\mathbf{u}) = 0$ having the shortest distance to the origin of the $\mathbf{u}$ space is determined by using an appropriate nonlinear optimization algorithm. This point is referred to as the design point or β-point, and has a distance β_{HL} to the origin of the $\mathbf{u}$ space. Third, the limit state $g_U(\mathbf{u}) = 0$ is approximated by a surface tangent to it at the design point. Let such limit states be $g_L(\mathbf{u}) = 0$ and $g_Q(\mathbf{u}) = 0$, which correspond to approximating surfaces as hyperplane (linear or first-order) and hyperparaboloid (quadratic or second-order), respectively. The probability of failure P_F (eqn (16)) is thus approximated by $Pr[g_L(\mathbf{u}) < 0]$ in FORM

and $Pr[g_Q(\mathbf{u}) < 0]$ in SORM. These first-order and second-order estimates $P_{F,1}$ and $P_{F,2}$ are given by[19,29–34]

$$P_{F,1} = \Phi(-\beta_{HL})$$
$$P_{F,2} \simeq \Phi(-\beta_{HL}) \prod_{i=1}^{N-1} (1 - \kappa_i \beta_{HL})^{-1/2} \tag{18}$$

where

$$\Phi(u) = \frac{1}{\sqrt{2\pi}} \int_{-\infty}^{u} \exp(-\tfrac{1}{2}\xi^2)\, d\xi \tag{19}$$

is the cumulative distribution function of a standard Gaussian random variable, and κ_is are the principal curvatures of the limit state surface at the design point. FORM/SORM are analytical probability computation methods. Each input random variable and the performance function $g(\mathbf{x})$ must be continuous. Depending on the solver for nonlinear programming, additional requirements regarding smoothness i.e. differentiability of $g(\mathbf{x})$ may be required. Further details of FORM/SORM equations are available in Ref. 19.

5.2 Monte Carlo simulation (MCS)

Consider a generic N-dimensional random vector $\mathbf{X}$ which characterizes uncertainty in all load and system parameters with the known joint distribution function $F_{\mathbf{X}}(\mathbf{x})$. Suppose $\mathbf{x}^{(1)}, \mathbf{x}^{(2)}, \ldots, \mathbf{x}^{(L)}$ are L realizations of input random vector $\mathbf{X}$ which can be generated independently. Rahman[19] provides a simple method to generate $\mathbf{X}$ from its known probability distribution. Let $g^{(1)}, g^{(2)}, \ldots, g^{(L)}$ be the output samples of $g(\mathbf{X})$ corresponding to the input $\mathbf{x}^{(1)}, \mathbf{x}^{(2)}, \ldots, \mathbf{x}^{(L)}$ that can be obtained by conducting repeated deterministic evaluations of the performance function in eqn (17). Define L_f as the number of trials which are associated with negative values of the performance function. Then, the estimate $P_{F,MCS}$ by simulation becomes

$$P_{F,MCS} = \frac{L_f}{L} \tag{20}$$

which approaches the exact failure probability P_F when L approaches infinity. When L is finite, a statistical estimate of the probability estimator may be needed. In general, the required sample size must be at least 10/Minimum(P_F, P_S) for a 30% coefficient of variation of the estimator.[41]

5.3 Importance sampling

In importance sampling, the random variables are sampled from a different probability density, known as the sampling density. The purpose is to generate more outcomes from the region of interest, e.g. the failure set $F = \{\mathbf{x}: g(\mathbf{x}) < 0\}$. Using information from FORM/SORM analyses, good sampling densities can be constructed. According to Hohenbichler,[39] the failure probability estimate $P_{F,IS}$ by importance sampling based on SORM improvement is given by

$$P_{F,IS} \simeq \Phi(-\beta_{HL}) \prod_{i=1}^{N-1} (1 - \kappa_i \psi(-\beta_{HL}))^{-1/2} \times \frac{1}{N_{IS}} \sum_{j=1}^{N_{IS}} \frac{\Phi(h_Q(\mathbf{w}_j))}{\Phi(\beta_{HL})} \exp\left[-\tfrac{1}{2}\psi(\beta_{HL}) \sum_{k=1}^{N-1} \kappa_k w_{k,j}^2 \right] \tag{21}$$

where $\psi(-\beta_{HL}) = \phi(-\beta_{HL})/\Phi(-\beta_{HL})$ with $\phi(\cdot)$ and $\Phi(\cdot)$ representing probability density and distribution functions, respectively, of a standard Gaussian random variable, $\mathbf{w}_j = \{w_{1,j}, w_{2,j}, \ldots, w_{N-1,j}\}^T$ is the jth realization of an $N-1$ dimensional independent Gaussian random vector $\mathbf{W}$ with the mean and variance of the ith component being zero and $1/[1 - \psi(-\beta_{HL})]$, $h_Q(\mathbf{w}_j)$ is the quadratic approximant in the form of a rotational hyperparaboloid, and N_{IS} is the sample size for importance sampling. Further details are available elsewhere.[19,35–40]

6 NUMERICAL APPLICATIONS

6.1 Description of the problem

For a numerical example, consider a TWC side riser pipe made of Type 304 stainless steel from a boiling water reactor (BWR) plant. The pipe had outer diameter $D_0 = 709{\cdot}17$ mm (27·92 in.), wall thickness $t = 33{\cdot}77$ mm (1·33 in.) [i.e. $R/t = 10$], and elastic modulus $E = 182{,}700$ MPa (26,500 ksi). These parameters were treated as deterministic variables since no significant statistical variabilities were found from their actual measurements. The operating temperature at BWR condition was assumed to be 288°C (550°F). The random parameters included crack size θ/π, yield strength σ_y, ultimate strength σ_u, Ramberg–Osgood constitutive parameters α and n, and fracture toughness parameters J_{Ic}, C and m. The statistical properties of these variables are described below.

6.1.1 Statistical characteristics of material properties

The samples of raw data for the stress–strain and J–resistance curves of a specific pipe material (e.g. Type 304 stainless steel) at 288°C (550°F) were obtained from Hiser and Callahan,[1] Wilkowski *et al.*,[2] Schmidt *et al.*,[3] Chopra *et al.*,[4] Landes *et al.*[5] and Van Der Sluys.[6] Each of these were then fitted with the eqns (1) and (2) to determine the constitutive model parameters α and n, and fracture toughness parameters, J_{Ic}, C and m. (This is a standard practice in the deterministic pipe fracture evaluations.) The

basic strength parameters, such as yield strength σ_y (0·2% offset) and ultimate strength σ_u, were determined as well. These provided the independent measurements of the random vectors $\{\sigma_y, \sigma_u\}^T$, and $\{J_{Ic}, C, m\}^T$ representing pipe material properties. Following standard statistical analyses, conducted in Rahman *et al.*,[45–47] Table 1 shows the mean and covariance for each of these random vectors. It was assumed that the joint probability distribution of each vector was lognormal. This was justified via comparisons with actual data in Fig. 7 which indicate that the marginal probability of each component of the above vectors follows lognormal distribution reasonably well. A Gaussian distribution also seems to be a good choice, but there are some concerns on the possible negative realizations of some of these positive random variables which have large coefficients of variation. Hence, **X** was modeled with lognormal probability although no rigorous proof was provided here to validate this assumption by comparing the multivariate joint probability distributions. Also, no correlations were permitted between the strength and toughness properties because each set of laboratory data did not always include simultaneous measurement of all properties. However, the components within each vector were correlated and their correlation characteristics were defined in the covariance matrices provided in Table 1. See Rahman[19] for the effects of correlation among random inputs on the piping reliability.

In general, a substantial amount of data is needed to obtain an accurate probability distribution of the material properties. The lognormal distribution of material properties was chosen based on the statistical analysis of a limited amount of data.[45–47] It is primarily used here to illustrate the probabilistic model developed in this study. If additional data are available or developed, they should be applied to verify this lognormal hypothesis. Also, it is useful to conduct some sensitivity calculations to probability distribution of input. For example, see Rahman[19] for variations in the input distribution of **X** and their effects on pipe fracture probability.

6.1.2 Statistical properties of initial flaw size

In order to perform probabilistic analysis, the probability distribution of initial crack size θ/π needs to be specified as well. In this example problem, it was assumed that the TWC crack was located in the base metal of the pipe with the anticipated cracking mechanism being intergranular stress corrosion cracking (IGSCC). During a recent study by the authors on probabilistic leak-before-break analysis (LBB), it was found that the leakage size flaw can be modeled by the lognormal or the truncated normal distributions.[45–47] The distribution parameters of this flaw size vary according to the leak-rate detection capability and applied normal stresses in the pipe. The analyses accounted for statistical variability of several crack morphology variables (e.g. surface roughness, number of turns or bends, path deviation factors, etc) of IGSCC crack, which can affect the leak rate through cracks typically found in nuclear piping. Detailed results of these analyses are available in Rahman *et al.*[45–47] Assuming that the initial crack is the LBB detectable flaw (leakage size crack), it was modeled here with a lognormal probability distribution. When the normal operating stress is 50% of service level-A stress (service level-A stress limit is equal to $1{\cdot}5S_m$, where S_m is the code-specified design stress defined in the ASME Section III, Appendix I)[48] and the leakage detection capability is 10 gpm, the mean value of θ/π is 0·16 with the coefficient of variation 9·69% for the side riser pipe considered in this example.[45–47] Comparisons of lognormal (and also Gaussian) distribution with simulated (computed) distribution of θ/π are also shown in Fig. 7. Further details can be obtained from Rahman *et al.*[45–47]

Table 1. Mean and covariance of material properties for type 304 stainless steel pipe at 288°C (550 F)

Random vector	Mean vector	Covariance matrix
$\begin{Bmatrix}\sigma_y\\ \sigma_u\end{Bmatrix}^a$	$\begin{Bmatrix}151{\cdot}526\\ 450{\cdot}632\end{Bmatrix}$	$\begin{bmatrix}220{\cdot}881 & 118{\cdot}615\\ 118{\cdot}615 & 652{\cdot}654\end{bmatrix}$
$\begin{Bmatrix}\alpha\\ n\end{Bmatrix}^b$	$\begin{Bmatrix}8{\cdot}942\\ 3{\cdot}615\end{Bmatrix}$	$\begin{bmatrix}10{\cdot}920 & -1{\cdot}202\\ -1{\cdot}202 & 0{\cdot}208\end{bmatrix}$
$\begin{Bmatrix}J_{Ic}\\ C\\ m\end{Bmatrix}^c$	$\begin{Bmatrix}1059{\cdot}56\\ 345{\cdot}087\\ 0{\cdot}652\end{Bmatrix}$	$\begin{bmatrix}2{\cdot}024\times10^5 & -58{\cdot}937 & -25{\cdot}530\\ -58{\cdot}937 & 1{\cdot}006\times10^4 & 6{\cdot}842\\ -25{\cdot}530 & 6{\cdot}842 & 0{\cdot}0242\end{bmatrix}$

[a] Both σ_y and σ_u are in MPa unit.
[b] α and n are dimensionless; $\sigma_0 = 152$ MPa; $E = 182700$ MPa (see eqn (1)).
[c] Both J_{Ic} and C are in kJ m^{-2} with $k = 1$ mm (see eqn (2)); m is dimensionless; Δa is to be expressed in mm.

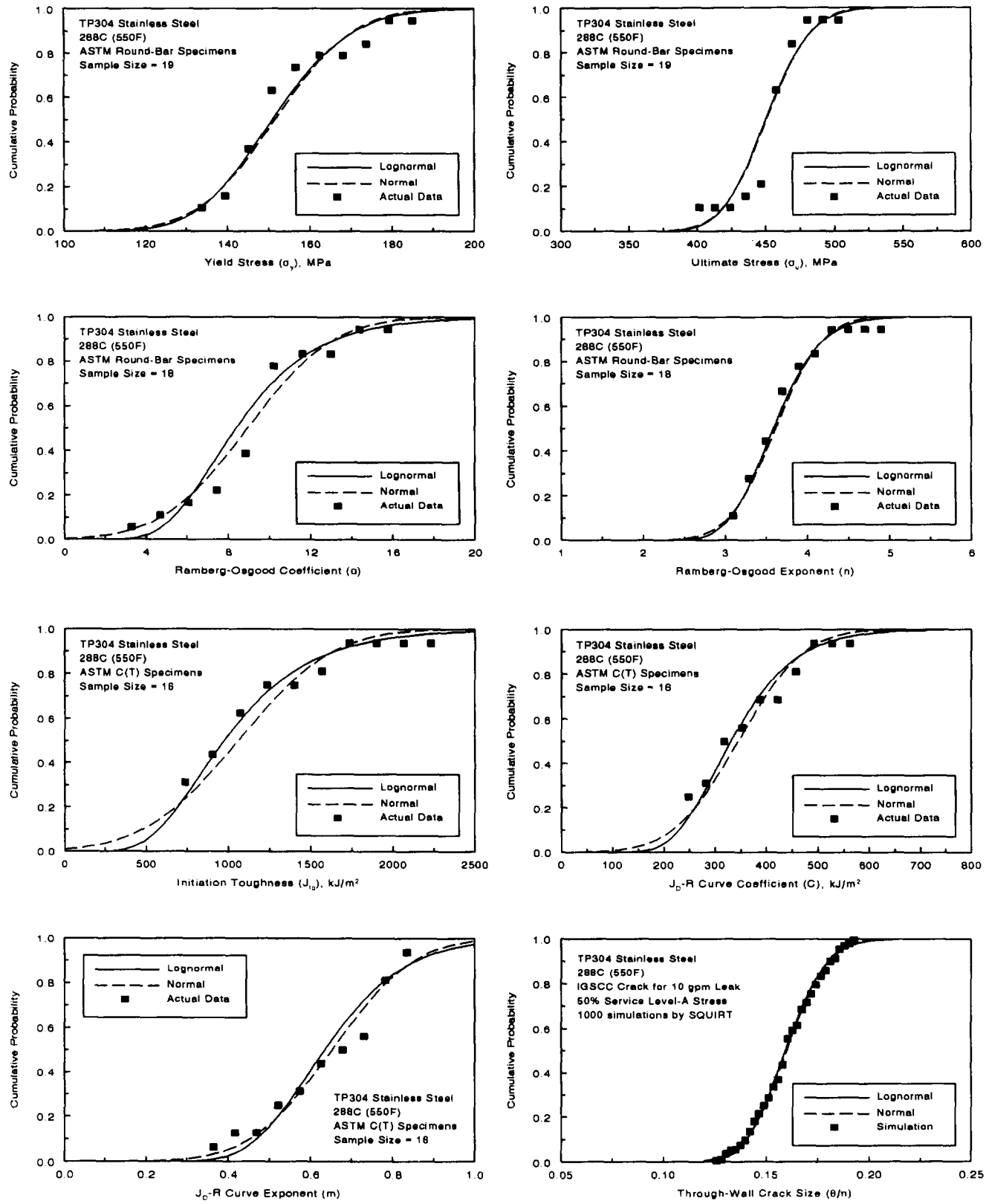

Fig. 7. Statistical characterization of random input variables.

The methods to generate samples of generic random vector **X**, which are needed in FORM/SORM and simulation analyses, require the Rosenblatt transformation to obtain the standard Gaussian vector **U**.[19,30–34] For special cases, when **X** is either correlated normal or correlated lognormal, the above transformation can be side-stepped by invoking the Cholesky decomposition of the covariance matrix. Further details on the sample generation of **X**, either generic or normal/lognormal, are available in Ref. 19.

6.2 Probabilistic characteristics of the *J*-integral

The second-order reliability method was applied to determine the probabilistic characteristics of the *J*-integral for the side riser pipe as a function of applied load. Figure 8 shows the computed probability densities $[f_J(j_0)]$ for several values of applied load $M = 1{\cdot}0$ MNm, $1{\cdot}25$ MNm and $1{\cdot}50$ Mnm. They were obtained by repeated FORM/SORM analysis for various thresholds of J, i.e. by calculating the probability in eqn (15) as a function of j_0 and then taking the numerical derivative of this probability with respect to j_0. As expected, the probability mass shifts to the right when the applied loads are higher. Also presented in the same figures are the corresponding histograms of *J*-integral developed by conducting direct Monte Carlo simulations for the same values of applied loads.

The sample size for each Monte Carlo analysis was 10,000. The results indicate that SORM can predict probabilistic characteristics of J with very good accuracy when compared with the Monte Carlo method for all values of applied load considered here.

Figure 9 shows the componential probability densities (as well as total) of *J*-integrals computed for several values of applied loads. Three load cases were considered and they were: $M = 0{\cdot}25$ MNm, $M = 0{\cdot}7$ MNm and $M = 1{\cdot}5$ MNm representing small, intermediate, and large load magnitudes, respectively. For each load, the probability densities of J_e, J_p and J $(=J_e + J_p)$ were computed by SORM. It appears that when the applied moment is small ($M = 0{\cdot}25$ MNm), the elastic component of J is much greater than the plastic component of J and hence, the fracture behavior is significantly governed by the elastic properties of pipe. On the other hand, when the applied load is large ($M = 1{\cdot}5$ MNm), the plastic component of J is more pronounced and thus nonlinear fracture mechanics become necessary to evaluate piping integrity. Finally, when the load magnitude is somewhat intermediate ($M = 0{\cdot}7$ MNm), both components of J are needed to predict the fracture behavior of pipes.

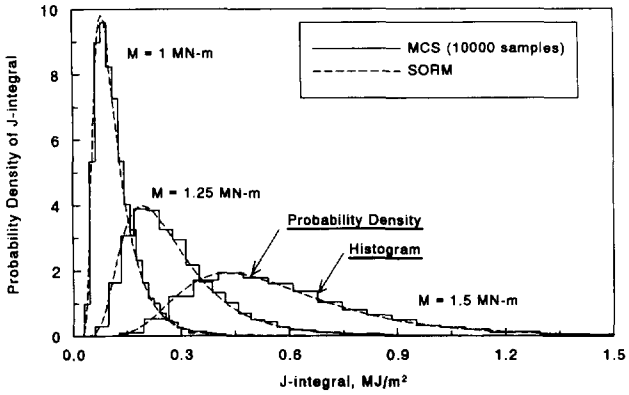

Fig. 8. Accuracy of SORM results in computing probabilistic characteristics of *J*.

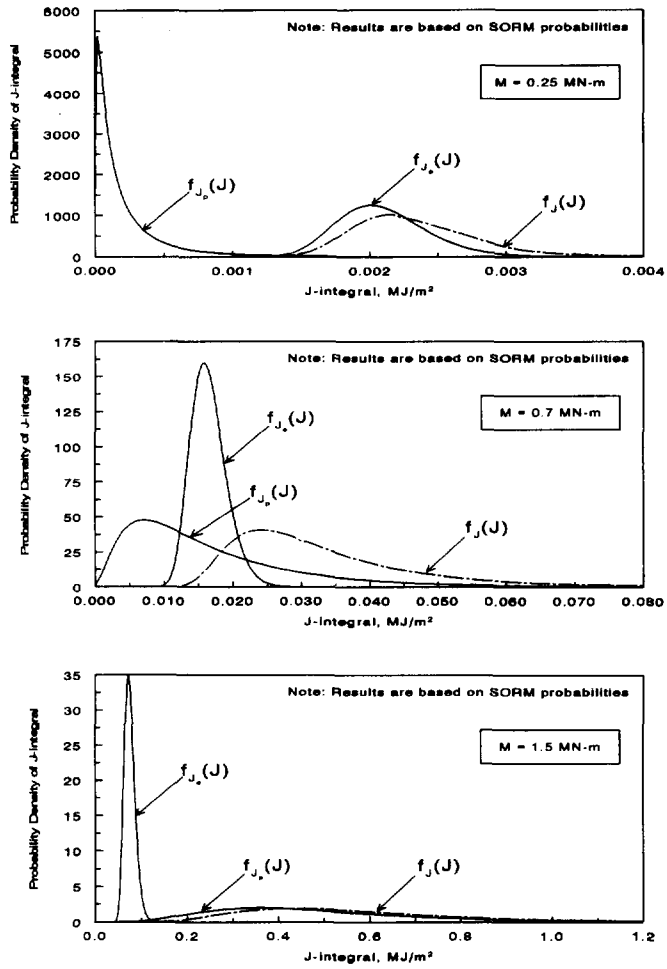

Fig. 9. Probabilistic characteristics of J_e-, J_p- and *J*-integrals for various loads.

6.3 Piping reliability assessment

Figure 10 shows the plots of failure probability P_F vs applied moment M for the side riser pipe obtained for several definitions of the failure load defined earlier. Various reliability methods, such as FORM and SORM, and simulation methods, such as IS and MCS, were used to determine the failure probability. They

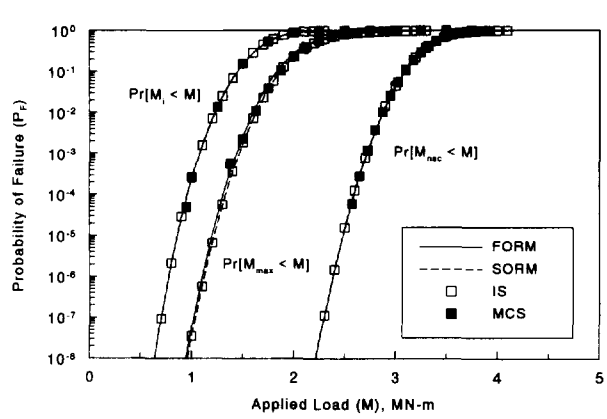

Fig. 10. Probability of failure by various methods.

all consistently indicate that P_F increases as M increases, and it approaches unity when M becomes very large. Compared with the failure probability due to the pipe instability, the failure probabilities based on the initiation of crack growth and net-section-collapse are found to be higher and lower, respectively. Unless there is sufficient evidence that the pipe will fail with a limit-load criterion, an analysis based on the net-section-collapse load (without any safety margin) may overpredict the reliability of pipes significantly. However, further studies are needed to verify this finding and determine if, indeed, this is a general trend.

Figure 10 also shows that the results obtained by the approximate methods, e.g. FORM and SORM provide satisfactory probability estimates when compared with the results from importance sampling and MCS methods. No meaningful differences are found between the results of FORM and SORM and their probability estimates are virtually identical. During the performance of MCS, the sample size was varied according to the level of probability being estimated. In all cases, the sample size was targeted to be $10/\text{Min}(P_F, P_S)$ [with a minimum of 500] for obtaining a 30% coefficient of variation of the probability estimator.

Figure 11 exhibits the relative effort and computational expenses required to determine above solutions by FORM, SORM, IS, and MCS methods. They were measured in terms of central processing units (CPU) by executing computer codes for each of these methods. The plots in this figure show how the ratio of CPU time required by FORM, SORM, and IS (the CPU ratio is defined as the ratio of the CPU by each of these methods and the CPU by MCS) varies with the range of probability estimates made in this study. It appears that for values of failure probability approaching 1, the CPU ratio also approaches 1 implying that the computational effort by each of these four methods is very similar. However, when the failure probabilities are smaller, a significant amount of CPU time can be saved by using FORM, SORM, and IS methods instead of using MCS. A computational advantage in the order of 10^{-6} times the CPU time required by MCS was observed in performing these pipe specific probability calculations. Similar efficiency of FORM/SORM was also reported by Riesch–Oppermann and Bruckner–Foit for other probabilistic fracture-mechanics evaluations.[44] Also, the differences in CPU times consumed by FORM, SORM, and IS analyses are quite negligible when compared with the magnitudes of CPU time required by MCS. Clearly, the FORM/SORM algorithms and importance sampling method are more efficient than the direct MCS and are far superior particularly when the failure probabilities are in the lower range.

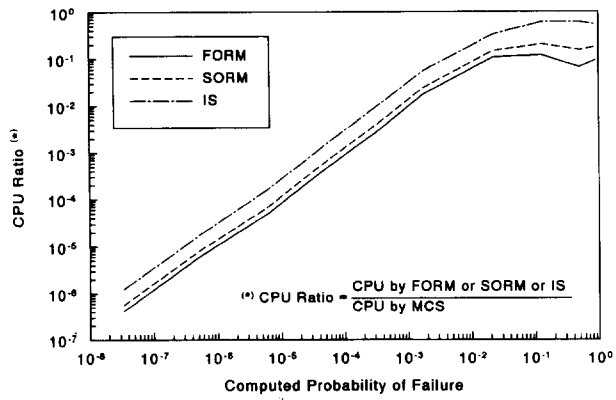

Fig. 11. Computational efficiency of FORM/SORM and importance sampling.

7 SUMMARY AND CONCLUSIONS

A probabilistic model was developed for fracture analysis of circumferential through-walled-cracked pipes subject to bending loads. It involves elastic–plastic finite element analysis for estimating energy release rates, J-tearing theory for characterizing ductile fracture, and standard structural reliability methods for conducting probabilistic analysis. The evaluation of the J-integral is based on the deformation theory of plasticity and power-law idealizations of stress–strain and fracture toughness curves. This allows the J-integral to be expressed in terms of non-dimensional influence functions that depend on crack size, pipe geometry, and material hardening constant. New equations were developed to represent these influence functions. The validity of the proposed equations for predicting crack driving force in a TWC pipe was evaluated by comparing with available results in the literature.

FORM/SORM and simulation methods were formulated to determine the probabilistic characteristics of the J-integral for a circumferential TWC pipe as a function of applied bending moment. The same methods were used later to compute the failure probability of the cracked pipes. Several failure criteria associated with crack initiation, unstable crack growth, and net-section-collapse were used to determine such probabilities. Numerical applications are provided to illustrate the proposed methodology. Nuclear piping made of Type 304 stainless steel (side riser pipe) from a boiling water reactor plant was chosen to evaluate its probabilistic performance. The results showed that:

- Current reliability methods, such as FORM and SORM, provided accurate probabilistic characteristics of J-integrals and failure loads for TWC pipes under bending with much less computational effort when compared with those obtained by direct MCS. A computational speedup in the order of 10^{-6} times the CPU time consumed by MCS was observed in performing pipe specific probability calculations.

Similar accuracy and computational efficiency were also demonstrated by the importance sampling method.

- The failure probabilities due to the exceedance of initiation load and net-section-collapse load were higher and lower, respectively, when compared with those due to the exceedance of maximum load of a TWC pipe. Large differences may exist in the results produced by each of the three failure criteria, especially when the applied load levels are smaller for which failure probabilities are also smaller. Unless there is adequate evidence that the pipe will fail with a limit-load criterion, an analysis based on net-section-collapse load (without any margin) may overpredict the reliability of a piping system significantly. However, further studies are needed to verify this finding and determine whether this is a general trend.

REFERENCES

1. Hiser, A. L. & Callahan, G. M., *A User's Guide to the NRC's Piping Fracture Mechanics Database (PIFRAC)*, NUREG/CR-4894, U.S. Nuclear Regulatory Commission, Washington, D.C., 1987.
2. Wilkowski, G. M., *et al., Degraded Piping Program—Phase II*, Semiannual Reports from March 1984 to January 1985, NUREG/CR-4082, Vols 1–8, U.S. Nuclear Regulatory Commission, Washington, D.C., 1985–1989.
3. Schmidt, R. A., Wilkowski, G. M. & Mayfield, M. E., The International Piping Integrity Research Group (IPIRG) Program—an overview. *Transactions of the 11th International Conference on Structural Mechanics in Reactor Technology, Vol. G2: Fracture Mechanics and Non-Destructive Evaluation—2*, Tokyo, Japan, August 1991, pp. 177–188.
4. Chopra, O. K., Sather, A. & Bush, L. Y., *Long-Term Embrittlement of Cast Duplex Stainless Steels in LWR Systems*, Semiannual Report, NUREG/CR-4744, Vol. 4, No. 2, U.S. Nuclear Regulatory Commission, Washington, D.C., June 1991.
5. Landes, J. D., McCabe, D. E. & Ernst, H. A., Elastic–plastic methodology to establish *R* curves and sustainability criteria. Semiannual Report on EPRI Contract no. RP1238-2, July 1983 to December 1983, Westinghouse R&D Center, July 1984.
6. Van Der Sluys, W. A., Toughness of ferritic piping steels. Final Report, EPRI NP-6264, Electric Power Research Institute, Palo Alto, CA, 1988.
7. Rice, J. R., A path-independent integral and the approximate analysis of strain concentration by notches and cracks. *Journal of Applied Mechanics*, 1968, **35,** 376–386.
8. Hutchinson, J. W., Fundamentals of the phenomenological theory of nonlinear fracture mechanics. *Journal of Applied Mechanics*, 1982, **49,** 103–107.
9. Rice, J. R. & Rosengren, G. F., Plane strain deformation near a crack-tip in a power-law hardening material. *Journal of the Mechanics and Physics of Solids*, 1968, **16,** 1–12.
10. Hutchinson, J. W., Singular behavior at the end of a tensile crack in a hardening material. *Journal of the Mechanics and Physics of Solids*, 1968, **16,** 13–31.
11. Paris, P. C., Tada, H., Zahoor, A. & Ernst, H., *The Theory of Instability of the Tearing Mode of Elastic–Plastic Crack Growth.* ASTM STP 668, American Society for Testing and Materials, Philadelphia, PA, 1979, pp. 5–36.
12. Shih, C. F. & Hutchinson, J. W., Fully plastic solutions and large-scale yielding estimates for plane stress crack problems. *Journal of Engineering Materials and Technology*, **98,** 1976, 289–295.
13. Kumar, V., German, M. D. & Shih, C. F., *An Engineering Approach for Elastic–Plastic Fracture Analysis.* EPRI/NP-1931, Electric Power Research Institute, Palo Alto, CA, 1981.
14. Kumar, V., German, M., Wilkening, W., Andrews, W., deLorenzi, W. & Mowbray, D., *Advances in Elastic–Plastic Fracture Analysis.* EPRI/NP-3607, Electric Power Research Institute, Palo Alto, CA, 1984.
15. Gilles, P. & Brust, F. W., Approximate fracture methods for pipes—Part 1: theory. *Nuclear Engineering and Design*, 1992, **127,** 1–27.
16. Brust, F., Rahman, S. & Ghadiali, N., Elastic–plastic analysis of small cracks in tubes. *Journal of Offshore Mechanics and Arctic Engineering*, 1995, **117**(1) 57–62; also available in the *Proceedings of the Offshore Mechanics and Arctic Engineering*, Calgary, Canada, June 1992.
17. *ABAQUS User's Guide and Manual*, Versions 4.6, 4.7, and 5.0. Hibbitt, Karlsson and Sorenson, 1993.
18. Brust, F. W., Scott, P., Rahman, S., Ghadiali, N., Kilinski, T., Francini, B., Marschall, C. W., Mura, N., Krishnaswamy, P. & Wilkowski, G. M., *Assessment of Short Through-Wall Circumferential Cracks in Pipes—Experiments and Analysis.* NUREG/CR-6235, U.S. Nuclear Regulatory Commission, Washington, D.C., April 1995.
19. Rahman, S., A stochastic model for elastic–plastic fracture analysis of circumferential through-wall-cracked pipes subject to bending. *Engineering Fracture Mechanics*, 1995, **52**(2) 265–288.
20. Sanders, J. L. Jr, Circumferential through-cracks in cylindrical shells under tension. *Journal of Applied Mechanics*, 1982, **49,** 103–107.
21. Sanders, J. L. Jr, Circumferential through-crack in a cylindrical shell under combined bending and tension. *Journal of Applied Mechanics*, 1983, **50,** 221.
22. Klecker, R., Brust, F. W. & Wilkowski, G. M., *NRC Leak-Before-Break (LBB.NRC) Analysis Method for Circumferentially Through-Wall Cracked Pipes Under Axial Plus Bending Loads.* NUREG/CR-4572, U.S. Nuclear Regulatory Commission, Washington, D.C., 1986.
23. Zahoor, A., Closed form expressions for fracture mechanics analysis of cracked pipes. *Journal of Pressure Vessel Technology*, 1985, **107.**
24. Wilkowski, G., Brust, F., Francini, R., Ghadiali, N., Kilinski, T., Krishmaswamy, P., Landow, M., Marschall, C. W., Rahman, S. & Scott, P., *Short Cracks in Piping and Piping Welds.* Semiannual Reports, NUREG/CR-4599, BMI-2173, Vols 1, 2 and 3, Nos 1 and 2, U.S. Nuclear Regulatory Commission, Washington, D.C., 1990–1994.
25. Rahman, S., Wilkowski, G. & Brust, F., Fracture analysis of full-scale pipe experiments on stainless steel flux welds. *Nuclear Engineering and Design*, 1996, **160,** 77–96.
26. Rahman, S., Wilkowski, G. & Brust, F., Analysis of full-scale pipe fracture experiments on stainless steel flux welds. *Proceedings of the 1994 ASME Pressure Vessels and Piping Division Conference*, Minneapolis, Minnesota, June 1994.

27. Press, W. H., Flannery, B. P., Teukolsky, S. A. & Vetterling, W. T., *Numerical Recipes*, Cambridge University Press, New York, 1990.
28. Kanninen, M. F. *et al.*, *Mechanical Fracture Predictions for Sensitized Stainless Steel Piping with Circumferential Cracks*, EPRI/NP-192, Electric Power Research Institute, Palo Alto, CA, 1976.
29. Hasofer, A. M. & Lind, N. C., An exact and invariant first-order reliability format. *Journal of Engineering Mechanics, ASCE*, 1974, **100**(EM1) 111–121.
30. Fiessler, B., Neumann, H. J. & Rackwitz, R., Quadratic limit states in structural reliability. *Journal of Engineering Mechanics, ASCE*, **105**(EM4), 661–676.
31. Rackwitz, R. & Fiessler, B., Structural reliability under combined random load sequences. *Computers & Structures*, 1978, **9**, 484–494.
32. Madsen, H. O., Krenk, S. & Lind, N. C., *Methods of Structural Safety*. Prentice-Hall, Englewood Cliffs, New Jersey, 1986.
33. Hohenbichler, M., New light on first- and second-order reliability methods. *Structural Safety*, 1987, **4**, 267–284.
34. Breitung, K., Asymptotic approximation for multinormal integrals. *Journal of Engineering Mechanics, ASCE*, 1984, **110**(3), 357–366.
35. Fu, G. & Moses, F., A sampling distribution for system reliability applications. *Proceedings of the First IFIP WG 7.5 Working Conference on Reliability and Optimization of Structural Systems*, Aalborg, Denmark, 1987, pp. 141–155.
36. Harbitz, A., An efficient sampling method for probability of failure calculation. *Structural Safety*, 1986, **3**(1), 109–115.
37. Harbitz, A., Efficient and accurate probability of failure calculation by use of the importance sampling technique. *Proceedings of the 4th International Conference on Applications of Statistics and Probability in Soil and Structural Engineering*, Florence, Italy, 1983.
38. Ibrahim, Y. & Rahman, S., Reliability analysis of uncertain dynamic systems using importance sampling. *Proceedings of the Sixth International Conference on Applications of Statistics and Probability in Civil Engineering*, Mexico City, Mexico, 1991.
39. Hohenbichler, M., Improvement of second-order reliability estimates by importance sampling. *Journal of Engineering Mechanics, ASCE*, 1988, **114**(12), 2195–2199.
40. Melchers, R. E., Efficient Monte Carlo probability integration. Report no. 7, Dept. of Civil Engineering, Monash University, Australia, 1984.
41. Rubinstein, R. Y., *Simulation and the Monte Carlo Method*. Wiley, New York, 1981.
42. Yagawa, G. & Ye, G.-W., A probabilistic fracture mechanics analysis for cracked pipe using 3-D model. *Reliability Engineering and System Safety*, 1993, **41**, 189–196.
43. Ye, G.-W., Yagawa, G. & Yoshimura, S., Probabilistic fracture mechanics analysis based on three-dimensional *J*-integral database. *Engineering Fracture Mechanics*, 1993, **44**, 887–893.
44. Riesch-Oppermann, M. & Bruckner-Foit, A., First- and second-order approximations of failure probabilities in probabilistic fracture mechanics. *Reliability Engineering and System Safety*, 1988, **23**, 183–194.
45. Rahman, S., Wilkowski, G. & Ghadiali, N., Pipe fracture evaluations for leak-rate detection: probabilistic models. *Proceedings of the ASME Pressure Vessels and Piping Division Conference*, PVP-Vol. 266, Creep, Fatigue Evaluation, and Leak-Before-Break Assessment, Denver, Colorado, July 1993.
46. Rahman, S., Wilkowski, G. & Ghadiali, N., Pipe fracture evaluations for leak-rate detection: applications to BWR and PWR piping. *Proceedings of the ASME Pressure Vessels and Piping Division Conference*, PVP-Vol. 266, Creep, Fatigue Evaluation, and Leak-Before-Break Assessment, Denver, Colorado, July 1993.
47. Rahman, S., Ghadiali, N., Paul, D. & Wilkowski, G., Probabilistic pipe fracture evaluations for leak-rate-detection applications, NUREG/CR-6004, U.S. Nuclear Regulatory Commision, Washington, D.C., April 1995.
48. 1989 Addenda ASME Boiler & Pressure Vessel Code—Section III, Article NB-3642.

APPENDIX A: COEFFICIENTS A_i, B_i AND C_{ij} FOR F- AND h_1-FUNCTIONS

A.1 Coefficients A_i and B_i

Let $\mathbf{A} = \{A_1, A_2, A_3\}^T$ and $\mathbf{B} = \{B_1, B_2, B_3, B_4\}^T$ be two vectors with the coefficients A_i and B_i as their components, respectively. **A** and **B** are given by[19]

$$\begin{aligned}\mathbf{A} &= \{0{\cdot}006215 \quad 0{\cdot}013304 \quad -0{\cdot}018380\}^T \\ \mathbf{B} &= \{175{\cdot}577 \quad 91{\cdot}69105 \quad -5{\cdot}53806 \quad 0{\cdot}15116\}^T\end{aligned} \tag{A1}$$

A.2 Coefficients C_{ij}

Let $\mathbf{C} = [C_{ij}]$, $i, j = 0, 1, 2, 3$, be a matrix with the coefficients C_{ij} as its components. **C** is given by[19]

$R/t = 5$

$$\mathbf{C} = \begin{bmatrix} 3{\cdot}74009 & 1{\cdot}43304 & -0{\cdot}10216 & 0{\cdot}002297 \\ -0{\cdot}19759 & -10{\cdot}19727 & -0{\cdot}45312 & 0{\cdot}04989 \\ 36{\cdot}42507 & 17{\cdot}03413 & 3{\cdot}36981 & -0{\cdot}21056 \\ -70{\cdot}4846 & -14{\cdot}69269 & -2{\cdot}90231 & 0{\cdot}15165 \end{bmatrix} \tag{A2}$$

$R/t = 10$

$$\mathbf{C} = \begin{bmatrix} 3{\cdot}39797 & 1{\cdot}31474 & -0{\cdot}07898 & 0{\cdot}00287 \\ -3{\cdot}07265 & 4{\cdot}34242 & -2{\cdot}48397 & 0{\cdot}11476 \\ 131{\cdot}7381 & -79{\cdot}02833 & 16{\cdot}18829 & -0{\cdot}66912 \\ -234{\cdot}6221 & 117{\cdot}0509 & -20{\cdot}30173 & 0{\cdot}79506 \end{bmatrix} \tag{A3}$$

$R/t = 20$

$$\mathbf{C} = \begin{bmatrix} 4{\cdot}07828 & -1{\cdot}55095 & 0{\cdot}67206 & -0{\cdot}04420 \\ -18{\cdot}21195 & 69{\cdot}92277 & -18{\cdot}41884 & 1{\cdot}11308 \\ 357{\cdot}4929 & -453{\cdot}1582 & 108{\cdot}0204 & -6{\cdot}56651 \\ -602{\cdot}7576 & 617{\cdot}9074 & -144{\cdot}9435 & 8{\cdot}90222 \end{bmatrix} \tag{A4}$$